Image-Guided Microbiopsy for Multimodal Skin-Ageing Classification: Clinical Feasibility, Imaging Phenotyping, and Biomarker Performance

Tarl Prow , Iaza Hussain , Miko Yamada *

Posted Date: 28 April 2026

doi: 10.20944/preprints202604.2019.v1

Keywords: microbiopsy; skin diagnostics; medical imaging; dermoscopy; wrinkle analysis; qPCR; biomarkers; ROC; classification; TGFBI; CIART; FOXQ1

 doi:10.20944/preprints202604.2019.v1

Article

Image-Guided Microbiopsy for Multimodal Skin-Ageing Classification: Clinical Feasibility, Imaging Phenotyping, and Biomarker Performance

Tarl Prow [1], Iaza Hussain [2] and Miko Yamada [1,*]

[1] Skin Research Center, Hull York Medical School, University of York, UK

[2] University Hospital of Derby and Burton Foundation Trust, UK

* Correspondence: miko.yamada@york.ac.uk

Abstract

Background/Objectives: Microbiopsy enables minimally invasive molecular sampling of skin, but diagnostic use will likely depend on integrating molecular readouts with imaging-based phenotype context. This manuscript frames the supplied Beiersdorf–UniSA/Prow volunteer study as a proof-of-concept diagnostic workflow for skin ageing and removes the ancillary shipping experiment to focus on clinical feasibility and classifier performance. Methods: Thirty volunteers were recruited into younger (20–30 years, n=15) and older (60–70 years, n=15) cohorts. Clinical photographs, dermoscopic images, skin-mold impressions, and inner-arm microbiopsy samples were collected. A 46-gene TaqMan qPCR panel was analyzed, with candidate biomarkers assessed for detectability, between-group separation, intra- versus interindividual variation, and receiver operating characteristic (ROC) performance. The manuscript was reconstructed from the supplied presentation and should therefore be regarded as a submission-ready draft derived from the available source material. Results: Pre- and post-procedure images showed only small punctate marks after sampling, supporting clinical feasibility of repeated, image-guided microbiopsy. Skin-surface roughness measures derived from mold imaging separated the younger and older cohorts on both displayed metrics ($p<0.0001$). Of 46 assayed genes, 43 were detected in at least one volunteer sample. TGFBI, CIART, and FOXQ1 were highlighted as the strongest age-associated markers. Single-gene ROC analysis ranked TGFBI (AUC 0.76), CIART (AUC 0.75), and FOXQ1 (AUC 0.73) highest. A three-gene model combining TGFBI, CIART, and FOXQ1 reached AUC 0.81 with sensitivity, specificity, positive predictive value, and negative predictive value all reported as 0.80. An exploratory four-gene model reached AUC 0.84, specificity 0.93, sensitivity 0.80, negative predictive value 0.82, and positive predictive value 0.92; the identity of the fourth marker should be confirmed from the original analytical files before submission. Conclusions: The available data support image-guided microbiopsy as the molecular component of a multimodal skin-ageing diagnostic workflow. Imaging supplies visual and roughness-based phenotype context, while a compact qPCR signature provides molecular discrimination. The study currently supports a clinically oriented proof-of-concept and justifies prospective validation with locked statistics, explicit ethics documentation, and source-verified standalone figures.

Keywords: microbiopsy; skin diagnostics; medical imaging; dermoscopy; wrinkle analysis; qPCR; biomarkers; ROC; classification; TGFBI; CIART; FOXQ1

1. Introduction

Minimally invasive diagnostics are increasingly attractive in dermatology because they can be repeated, paired with serial imaging, and deployed with less procedural burden than conventional punch biopsy. In parallel, skin ageing research has increasingly combined molecular, structural, and imaging-derived end points to capture both biological and phenotypic dimensions of tissue ageing [5,7–11].

 doi:10.20944/preprints202604.2019.v1

Microbiopsy provides sub-millimetre tissue sampling with a small visible footprint and has therefore emerged as a potential bridge between phenotype imaging and molecular testing [1–4,12,13]. Prior work has shown that microbiopsy and related microneedle-based sampling approaches can support gene-expression analysis while minimizing visible injury and facilitating repeat sampling, which is essential for longitudinal and image-guided dermatologic applications [1–4,12,13].

The key question is not simply whether RNA can be recovered from microbiopsy tissue, but whether an image-guided microbiopsy workflow can support clinically meaningful classification of younger and older skin. The strongest evidence available in the supplied material lies in three aligned layers: representative pre- and post-procedure images showing limited visible trauma, roughness-based skin imaging that discriminates between age groups, and targeted qPCR biomarkers with multigene ROC performance that suggest diagnostic potential. The biological rationale for age-associated molecular discrimination is supported by prior work showing transcriptomic changes with age in human skin and other tissues [5,6].

Accordingly, the study emphasizes a multimodal diagnostic concept in which imaging defines the phenotype context and microbiopsy supplies the molecular classifier. This framing is consistent with broader trends in dermatologic diagnostics, where multimodal and noninvasive imaging are increasingly used to improve lesion characterization and clinical decision-making, and with reporting standards that encourage transparent evaluation of diagnostic accuracy [7–9,14–16].

2. Materials and Methods

2.1. Volunteer Cohort and Clinical Procedures

Thirty Caucasian female volunteers were recruited into two age groups: 20–30 years (n=15) and 60–70 years (n=15). The approval was obtained by University Human Ethic Committee (Protocol No: 200017). Clinical photographs and dermoscopic images were acquired for each participant, and skin-mold impressions were collected by using a VISIA, Canfield, Inc, USA for wrinkle and roughness analysis. Six microbiopsies were obtained from the inner arm of each volunteer, and samples for the reported molecular analyses were preserved in RNALater prior to downstream processing.

In the diagnostic framing used here, clinical and dermoscopic images are treated as part of the intended test workflow because they document the sampled site, show the limited visible footprint of the procedure, and provide contextual phenotype information alongside the molecular result.

Table 1. shows the summary of study workflow and diagnostic interpretation.

Workflow layer	Study input	Evidence in supplied dataset	Diagnostic role
Clinical/dermoscopic imaging	Pre- and post-microbiopsy photographs	Representative younger and older volunteer images plus age-group plot	Documents sampled site, shows limited visible footprint, and provides subject-level phenotype context
Surface-topography imaging	Skin-mold wrinkle/roughness analysis	Both displayed roughness metrics separated cohorts at $p<0.0001$	Quantitative phenotype layer complementary to molecular testing
Microbiopsy qPCR	Targeted 46-gene panel	43/46 genes detectable; TGFBI, CIART, and FOXQ1 prioritized	Core molecular classifier component
Classifier analysis	ROC-based single-gene and multigene models	Three-gene panel AUC 0.81; exploratory four-gene panel AUC 0.84	Prototype diagnostic performance summary

2.2. Skin Imaging and Surface-Topography Analysis

Representative volunteer images show pre- and post-microbiopsy skin appearance in one younger and one older participant. Skin-mold impressions were further analyzed for roughness-based metrics, both of which separated the age cohorts at $p<0.0001$ in the supplied results. These methods align with prior work showing that skin surface topography, roughness, and dermoscopic patterning provide measurable correlates of chronological and photoaging-related skin change [7–9].

These imaging outputs were interpreted as a quantitative phenotyping layer complementary to microbiopsy-derived molecular profiling.

 doi:10.20944/preprints202604.2019.v1

Table 2. Leading molecular classifier results reported in the presentation.

Model or marker	Detection	Reported performance	Interpretation
TGFBI	30/30	AUC 0.76	Best single-gene performer in supplied dataset
CIART	27/30	AUC 0.75	Strong single-gene discriminator
FOXQ1	28/30	AUC 0.73	Third-ranked single-gene discriminator
TGFBI + CIART + FOXQ1	Not separately stated	AUC 0.81; sensitivity 0.80; specificity 0.80; NPV 0.80; PPV 0.80	Good performance for compact three-gene panel
Three-gene panel + one UniSA/Prow marker	Fourth marker identity to be confirmed	AUC 0.84; sensitivity 0.80; specificity 0.93; NPV 0.82; PPV 0.92	Best reported model; source verification needed before submission

2.3. RNA Extraction and Targeted qPCR Panel

46-gene were selected as aging markers for TaqMan qPCR panel applied to the volunteer study samples. Of the 46 genes assayed, 43 were detected in at least one volunteer sample, whereas three were not detected in any volunteers. TGFBI, CIART, and FOXQ1 were highlighted as the principal age-associated genes showing between-group expression differences in the supplied analysis.

2.4. End Points and Statistical Reporting

Primary end points in this manuscript were: (i) clinical feasibility of microbiopsy as judged from pre- and post-procedure images; (ii) imaging-based cohort separation using skin roughness metrics; (iii) detectability and cohort discrimination for candidate qPCR biomarkers; and (iv) classifier performance using ROC analysis.

3. Results

3.1. Clinical Imaging Supports a Feasible, Minimally Invasive Sampling Workflow

Representative pre- and post-microbiopsy images from a 23-year-old participant and a 62-year-old participant show only small punctate post-procedure marks at the sampled inner-arm sites (**Figure 1**).

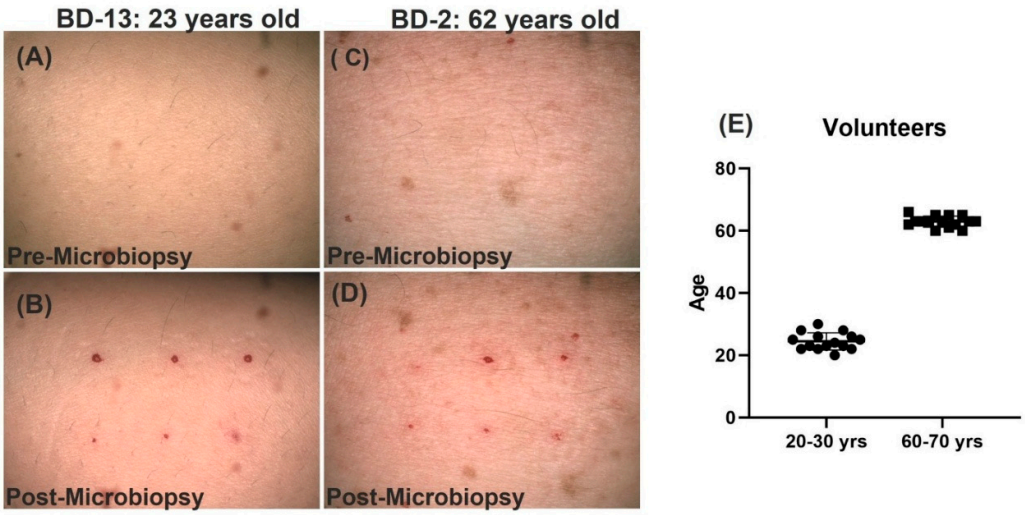

Figure 1. Representative skin appearance before and after microbiopsy sampling in younger and older adult volunteers. Representative clinical images show the skin surface before and after microbiopsy collection in two healthy volunteers from different age groups. Panels A–B show volunteer BD-13, a 23-year-old participant, and

 doi:10.20944/preprints202604.2019.v1

panels C–D show volunteer BD-2, a 62-year-old participant. Pre-procedure images demonstrate intact skin prior to sampling in the younger participant (A) and older participant (C). Post-procedure images show the same general sampling areas following microbiopsy collection in the younger participant (B) and older participant (D), with multiple small, punctate erythematous sampling sites visible at the skin surface.

The visual footprint was modest in both age groups, supporting the practicality of image-guided sampling in a clinical or translational workflow. The post-microbiopsy appearance is limited to localized pinpoint marks with mild surrounding redness, consistent with minimally invasive sampling. Panel E shows the age distribution of the volunteer cohorts, comparing participants aged 20–30 years with those aged 60–70 years. Each symbol represents an individual volunteer, with horizontal bars indicating the group mean and variability. The two cohorts are clearly separated by age, enabling comparison of microbiopsy outcomes between younger and older adult skin

The age-distribution plot presented alongside the images confirms appropriate separation between the younger and older cohorts.

3.2. Skin-Surface Roughness Imaging Differentiates Younger and Older Cohorts

Wrinkle and roughness analysis derived from skin-mold imaging separated the two age groups on both displayed metrics (**Figure 2**).

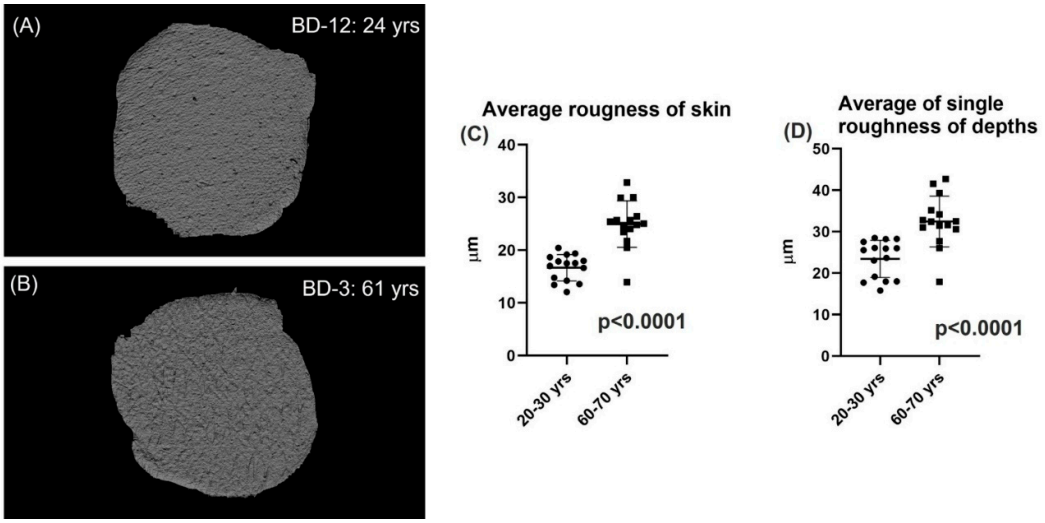

Figure 2. Increased skin surface roughness and depth variation in older adult volunteers. Representative three-dimensional surface reconstructions of microbiopsy-collected skin samples are shown for a younger adult volunteer, BD-12, 24 years old (A), and an older adult volunteer, BD-3, 61 years old (B). The older volunteer sample displays a more irregular surface texture compared with the younger volunteer sample. Quantitative analysis of skin surface topography showed that the average roughness of skin was significantly higher in volunteers aged 60–70 years compared with volunteers aged 20–30 years (C; $p < 0.0001$). Similarly, the average single roughness of depths was significantly increased in the older volunteer group relative to the younger group (D; $p < 0.0001$). Each symbol represents an individual volunteer, with circles indicating the 20–30-year age group and squares indicating the 60–70-year age group. Horizontal bars indicate the group mean with variability. These findings demonstrate age-associated increases in skin surface roughness and depth heterogeneity as measured from microbiopsy-derived skin surface profiles.

To assess whether microbiopsy samples could be used to evaluate skin surface architecture, skin surface topography was visualized from representative microbiopsy-derived samples obtained from younger and older adult volunteers. Representative surface reconstructions showed clear qualitative differences between age groups. The skin surface from the younger volunteer, BD-12, 24 years old, appeared comparatively smoother and more uniform, with less pronounced surface irregularity. In

 doi:10.20944/preprints202604.2019.v1

contrast, the sample from the older volunteer, BD-3, 61 years old, displayed a more uneven and textured surface, with visibly greater variation in surface contour. These representative images suggest that microbiopsy-derived skin samples preserve measurable surface features that can be used to evaluate age-related differences in skin microarchitecture. Quantitative analysis of skin surface roughness demonstrated a marked difference between the two age groups. Volunteers aged 20–30 years showed lower average skin roughness values, with most measurements clustering within a relatively narrow range. In contrast, volunteers aged 60–70 years exhibited higher average roughness values, indicating a more irregular skin surface in the older cohort.

The difference between age groups was statistically significant, with average skin roughness increased in the 60–70-year group compared with the 20–30-year group ($p < 0.0001$). This result indicates that aging is associated with a measurable increase in skin surface roughness, as captured using the microbiopsy-based surface analysis approach. In addition to overall surface roughness, the average single roughness of depths was quantified to assess variation in surface depth features. Similar to the average roughness measurement, younger volunteers showed lower depth-roughness values, while older volunteers showed higher values. The distribution of data points indicates that depth-associated roughness was consistently elevated in the older age group, although some interindividual variability was observed within both cohorts.

The increase in average single roughness of depths in the 60–70-year group was statistically significant compared with the 20–30-year group ($p < 0.0001$). These findings suggest that older skin not only has a rougher surface overall, but also displays greater heterogeneity in depth-related topographic features.

Together, both quantitative parameters demonstrated clear separation between the younger and older volunteer groups. The older cohort showed increased values for both average skin roughness and average single roughness of depths, consistent with the representative images showing a more irregular surface structure in older skin. These results indicate that microbiopsy-derived surface profiling can detect age-associated changes in skin architecture and may provide a minimally invasive approach for assessing structural features of skin aging.

Overall, the findings demonstrate that skin aging is associated with increased surface roughness and greater depth variation, and that these changes can be captured quantitatively from microbiopsy-derived samples.

3.3. TGFBI, CIART, and FOXQ1 Are Emerging as the Leading Markers

To determine which gene-expression targets were suitable for downstream analysis in microbiopsy-derived skin samples, candidate genes were grouped according to detection frequency (**Figure 3**).

The genes were categorized as detected in all samples, detected in more than 10 samples per group, detected in fewer than 10 samples per group, or not detected. This approach enabled prioritization of genes with reliable amplification across the sample set. The housekeeping genes GAPDH and ACTB were detected in all samples, supporting the quality and amplifiability of the microbiopsy-derived cDNA. Several candidate genes were also detected in all samples, including TGFBI, GSDMA, SERPINA3, APOD, TRIM15, and KLF6. The complete detection of these genes indicates that they are robustly measurable from microbiopsy-derived skin material and are suitable for comparative expression analysis. Among these, TGFBI was highlighted as a priority candidate for further evaluation. A larger subset of genes was detected in more than 10 samples per group, indicating moderate detection reliability. This group included EDN1, S100A9, TSC22D1, S100A8, PI3, IL22RA1, DUSP1, PMEL, SPON2, IL32, FOXQ1, SMTN, DDIT3, and CIART. Although these genes were not detected in every sample, their detection frequency was sufficient to support further consideration in downstream analyses. Notably, FOXQ1 and CIART were highlighted as candidate genes of interest, suggesting that they may provide useful discriminatory or biological information despite incomplete detection across all samples. A number of genes were detected in fewer than 10 samples per group, including S100A7, SERPINB4, IL6, CHI3L2, IL27RA, IGSF10, GDA, LCN2,

 doi:10.20944/preprints202604.2019.v1

KRT6B, TNFAIP6, G0S2, TCHH, KLF2, KRT71, KRT86, KRT74, HEPHL1, CCL20, WDR66, CDKN2A, TRIM10, and PITX1. Because these genes were detected inconsistently, they are less suitable as standalone targets for reliable comparative analysis in this microbiopsy sample set. In addition, S100A7A, TNNT3, and ACSF2 were not detected, indicating that these transcripts were either absent, below the assay detection threshold, or not reliably measurable under the conditions used. Overall, the detection analysis demonstrated that microbiopsy-derived skin samples provide sufficient material for consistent measurement of several housekeeping and candidate genes. Genes detected in all samples, particularly TGFBI, showed the strongest technical reliability for downstream expression analysis. Genes detected in more than 10 samples per group, including FOXQ1 and CIART, may also be useful candidates, although their incomplete detection should be considered when interpreting group comparisons. In contrast, genes with low or absent detection were less suitable for further analysis in this dataset. These findings support a focused gene-selection strategy in which robustly detected targets are prioritized for biomarker evaluation and age-associated skin gene-expression profiling.

Detected all	detected >10 per group	Less than <10 per group	Not detected
GAPDH	EDN1	S100A7	S100A7A
ACTB	S100A9	SERPINB4	TNNT3
TGFBI*	TSC22D1	IL6	ACSF2
GSDMA	S100A8	CHI3L2	
SERPINA3	PI3	IL27RA	
APOD	IL22RA1	IGSF10	
TRIM15	DUSP1	GDA	
KLF6	PMEL	LCN2	
	SPON2	KRT6B	
	IL32	TNFAIP6	
	FOXQ1*	G0S2	
	SMTN	TCHH	
	DDIT3	KLF2	
	CIART*	KRT71	
		KRT86	
		KRT74	
		HEPHL1	
		CCL20	
		WDR66	
		CDKN2A	
		TRIM10	
		PITX1	

Figure 3. Detectability summary for the targeted 46-gene qPCR panel. The supplied analysis reports detection of 43 of 46 genes and highlights TGFBI, CIART, and FOXQ1 as the key age-associated markers. Reproduced from slide 9 of the supplied presentation.

3.4. Variation Analysis Supports Biological Discrimination Despite Sampling Heterogeneity

To determine whether skin microbiopsy samples provide sufficient material for downstream gene-expression analysis, cDNA yield was measured from individual microbiopsy-derived samples. Detectable cDNA was recovered from all samples analyzed, although the total amount of cDNA varied between microbiopsies (**Figure 4 (A)**).

 doi:10.20944/preprints202604.2019.v1

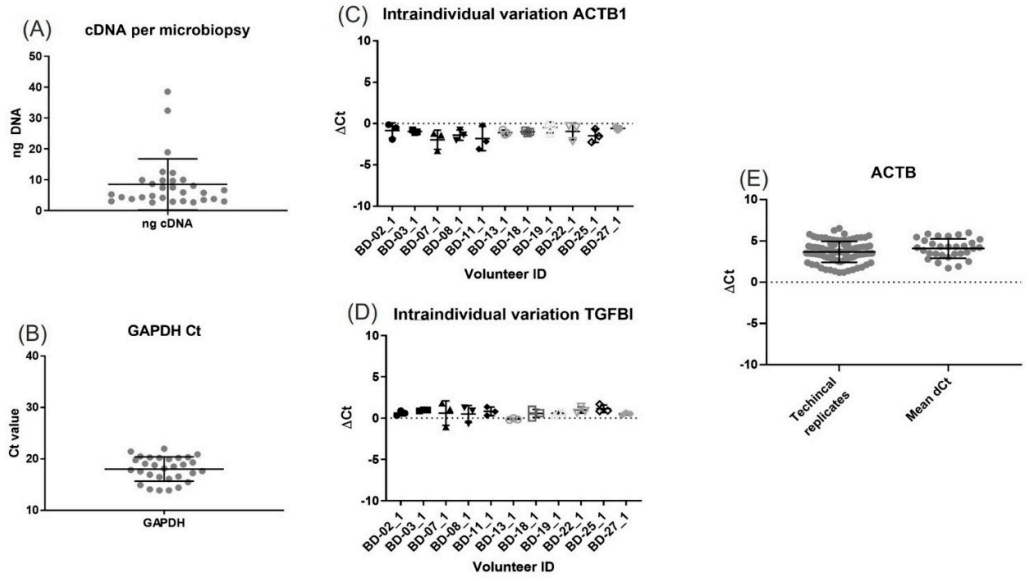

Figure 4. Microbiopsy samples yield sufficient cDNA for reproducible gene-expression analysis. Quantification of nucleic acid recovery and qPCR performance from individual microbiopsy samples. (A) Amount of cDNA obtained per microbiopsy, expressed as ng cDNA, showing detectable cDNA recovery across individual samples with some sample-to-sample variability. (B) GAPDH Ct values measured from microbiopsy-derived cDNA, demonstrating consistent amplification of the reference gene across samples. (C) Intraindividual variation in ACTB expression across repeated microbiopsy samples from individual volunteers, shown as ΔCt values for each volunteer ID. (D) Intraindividual variation in TGFBI expression across repeated microbiopsy samples from the same volunteer set, shown as ΔCt values. For panels C and D, each symbol represents an individual microbiopsy replicate, and grouped points indicate replicate measurements from the same volunteer. (E) Comparison of ACTB ΔCt values obtained from technical replicates versus mean dCt values, demonstrating comparable ACTB measurement consistency between replicate-level and averaged analyses. Horizontal bars indicate the group mean with variability. The dotted horizontal line marks ΔCt = 0. Overall, these data demonstrate that microbiopsy-derived material is suitable for reproducible downstream qPCR-based gene-expression assessment.

Most samples yielded relatively low but measurable quantities of cDNA, while a small number of samples produced higher yields, indicating some variability in sample recovery or tissue input across microbiopsies. Overall, the distribution of cDNA yield demonstrated that microbiopsy sampling can provide sufficient nucleic acid material for molecular analysis from minimally invasive skin samples. To assess whether the recovered material was suitable for quantitative PCR analysis, GAPDH Ct values were measured across microbiopsy-derived cDNA samples. GAPDH amplification was consistently detected, with Ct values clustering within a relatively narrow range across samples **(Figure 4(B))**. This indicates that the extracted and reverse-transcribed material was of adequate quality for qPCR and that microbiopsy-derived cDNA supported reproducible amplification of a housekeeping gene. The consistency of GAPDH Ct values further suggests that, despite variability in total cDNA yield, the samples were suitable for comparative gene-expression measurements.

Intraindividual variation was evaluated by comparing ACTB ΔCt values across repeated microbiopsy samples collected from the same volunteers. ACTB ΔCt values were generally clustered close to the zero-reference line for each volunteer, indicating limited variation among replicate microbiopsies from the same individual. Although some volunteers showed modest spread between replicate measurements, the overall distribution remained narrow. These findings suggest that ACTB expression measurements from microbiopsy-derived samples are reproducible within individuals and that repeated microbiopsies provide comparable qPCR readouts for this reference gene.

 doi:10.20944/preprints202604.2019.v1

To determine whether reproducibility extended beyond housekeeping genes, intraindividual variation was also assessed for TGFBI. Similar to ACTB, TGFBI ΔCt values were closely grouped within each volunteer, with most replicate measurements lying near the zero-reference line. The limited dispersion of ΔCt values across repeated microbiopsies indicates that TGFBI expression can be measured reproducibly from microbiopsy-derived cDNA. These results support the use of microbiopsy sampling for quantifying both reference and target gene expression in skin.

ACTB ΔCt values were further compared between technical replicates and mean dCt-based values (**Figure 4 (C**)). Technical replicate measurements showed a similar distribution to the averaged dCt values, with both groups clustering within a comparable ΔCt range. This indicates that qPCR technical variability was limited and that averaging replicate measurements did not substantially alter the overall ACTB expression profile. Together, these data demonstrate that the observed gene-expression patterns are not primarily driven by technical variability.

The variation-analysis slide shows expected heterogeneity in cDNA yield per microbiopsy and GAPDH Ct values, reflecting ordinary differences in sample capture and preparation (**Figure (D)**). Despite this, the reported dCt standard deviations indicate lower intraindividual than interindividual variation for the highlighted genes ACTB1 and TGFBI (0.68 vs. 1.18, and 0.58 vs. 0.86, respectively) **(Figure 4 (E)**).

These findings are consistent with a sampling workflow in which biological differences between participants remain measurable despite the small tissue volume obtained by microbiopsy.

3.5. Candidate Biomarker and Classifier Performance Support a Prototype Diagnostic Panel

To assess the ability of individual genes to distinguish between the comparison groups, receiver operating characteristic-based performance was evaluated using the area under the curve (AUC) (**Figure 5)**. A total of 20 candidate genes were included in the analysis (Figure 5).

Gene Name (detected/total)	AUC
TGFBI (30/30)	**0.76**
CIART (27/30)	0.75
FOXQ1 (28/30)	0.73
APOD	0.60
KLF6	0.59
PI3	0.59
GSDMA	0.58
TRIM15	0.58
SMTN	0.57
DUSP1	0.55
S100A8	0.54
DDIT3	0.53
EDN1	0.52
S100A9	0.51
PMEL	0.51
TSC22D1	0.50
IL32	0.50
SERPINA3	0.49
SPON2	0.48
IL22RA1	0.46

Figure 5. Receiver operating characteristic analysis of individual candidate biomarkers. TGFBI, CIART, and FOXQ1 show the strongest single-gene AUC values in the supplied dataset.

 doi:10.20944/preprints202604.2019.v1

For several genes, the number of samples in which the gene was detected is shown relative to the total number analyzed, indicating that some transcripts were not detected in every sample. Among the genes listed, AUC values ranged from 0.46 to 0.76, suggesting variable discriminatory performance across the candidate panel. Among all genes assessed, TGFBI demonstrated the strongest performance, with an AUC of 0.76. TGFBI was detected in 30 of 30 samples, indicating complete detection across the analyzed sample set. This combination of full detection and the highest AUC suggests that TGFBI was the most robust individual marker among the genes evaluated. An AUC of 0.76 indicates moderate discriminatory ability and supports TGFBI as a promising candidate transcript for distinguishing the study groups. Two additional genes showed relatively high AUC values. CIART had an AUC of 0.75 and was detected in 27 of 30 samples, while FOXQ1 had an AUC of 0.73 and was detected in 28 of 30 samples. These values were only slightly lower than the AUC observed for TGFBI, indicating that CIART and FOXQ1 also demonstrated moderate ability to separate the groups. However, unlike TGFBI, both CIART and FOXQ1 were not detected in all samples, which may affect their reliability as standalone biomarkers. Together, these three genes represented the best-performing markers in the panel, each achieving an AUC greater than 0.70. The remaining genes had lower AUC values, generally ranging from approximately 0.46 to 0.60. APOD showed an AUC of 0.60, while KLF6 and PI3 each had an AUC of 0.59. GSDMA and TRIM15 both showed AUC values of 0.58, and SMTN showed an AUC of 0.57. These genes demonstrated only modest separation between groups and are likely to have limited utility as individual classifiers. Genes with AUC values near 0.50, including TSC22D1 and IL32 both at 0.50, showed performance close to random classification. Similarly, SERPINA3, SPON2, and IL22RA1 had AUC values below 0.50, with IL22RA1 showing the lowest AUC at 0.46. These genes did not appear to provide meaningful discriminatory value in this analysis when considered individually. Overall, the AUC analysis identified TGFBI, CIART, and FOXQ1 as the strongest-performing candidate genes, with AUC values of 0.76, 0.75, and 0.73, respectively. Among these, TGFBI was the most favorable candidate because it combined the highest AUC with detection in all analyzed samples. In contrast, most other genes showed weak to minimal classification performance, with AUC values close to 0.50. These findings suggest that TGFBI, and to a lesser extent CIART and FOXQ1, may have potential as individual gene-expression markers, while the remaining genes may require combination with other markers or may be less informative for distinguishing the analyzed groups.

4. Discussion

The present dataset is most persuasive when interpreted as a clinically oriented, multimodal diagnostic proof-of-concept rather than as a purely cosmetic or exploratory biomarker study. That interpretation is consistent with contemporary views of skin ageing as a multidimensional process involving molecular, structural, and phenotypic change, and with current interest in combining minimally invasive molecular assays with noninvasive imaging in dermatology [5,7–11,14,17].

A central strength of the study is therefore the convergence of orthogonal evidence streams. The imaging results show that the two age groups are separable at the phenotype level, while the qPCR results indicate that a targeted molecular panel can discriminate between them at the biomarker level. Multimodal approaches are attractive in dermatology because each modality offsets the limitations of the others: visual and surface-topography data preserve spatial and morphologic context, whereas molecular assays can capture biology that may not yet be apparent clinically [9,15,17,18].

The volunteer photographs are especially important from a deployment perspective. Many otherwise promising molecular skin assays fail to become practical because the sampling procedure is too invasive, too conspicuous, or too difficult to repeat serially. By contrast, prior microbiopsy studies have emphasized minimal residual marking, feasibility across dermatologic applications, and compatibility with histologic or gene-expression endpoints, all of which support the translational logic of image-guided repeat sampling [1–4,12,13].

The roughness-imaging results further strengthen the diagnostic framing because they provide a phenotype layer that is not dependent on gene expression alone. The strong separation of the age

 doi:10.20944/preprints202604.2019.v1

groups on both roughness metrics is biologically plausible and concordant with previous studies linking skin surface topography, dermoscopic ageing features, and transcriptomic or cellular hallmarks of skin ageing [7–11,19,20].

The molecular results are also encouraging because they imply that individual microbiopsy samples can yield interpretable targeted qPCR data despite the small quantity of tissue obtained. The fact that 43 of 46 genes were detectable supports panel-level feasibility, while the emergence of TGFBI, CIART, and FOXQ1 as leading single-gene markers suggests that the assay is capturing biologically relevant age-associated variation. Although these specific markers will still require external validation, the broader concept is supported by prior gene-expression studies showing robust ageing-associated transcriptional differences in human skin, including in dermal and epidermal compartments and at single-cell resolution [6,10,11,18–20].

The variation analysis is another clinically relevant feature of the dataset. Small-volume tissue sampling inevitably introduces concern about heterogeneity in capture depth, local anatomy, and RNA yield. Here, however, intraindividual variation was lower than interindividual variation for the displayed markers, implying that biological signal can remain discernible despite sampling noise. That observation is important for future diagnostic development because it supports repeated sampling designs and serial response monitoring. It also underscores the need for future studies to follow formal diagnostic-accuracy reporting frameworks such as STARD when locking classifier thresholds, defining intended use, and validating performance across cohorts [15,16].

At the same time, the study should remain careful and transparent about the current level of evidence. The cohort is small, the classifier has not yet been externally validated. These limitations do not negate the signal; rather, they locate the work appropriately as an early translational study positioned between assay feasibility and formal diagnostic validation [15,16].

These limitations also point directly to the next development steps. A follow-up study should prospectively lock the biomarker panel, define the intended use of the assay, pre-specify statistical thresholds, and evaluate performance in an independent cohort enriched for clinically relevant confounders such as sex, phototype, UV exposure history, anatomic site, and inflammatory skin status. Future studies could also integrate richer imaging modalities, as multimodal imaging is increasingly being evaluated across dermatology to improve diagnostic accuracy and workflow performance [14,17].

Overall, the study supports a clinically attractive concept: microbiopsy can function as the molecular backbone of a multimodal skin diagnostic workflow rather than as an isolated laboratory assay. That is a meaningful translational position because dermatology already depends heavily on visual assessment, and molecular tools are most likely to succeed when they augment rather than replace phenotype-rich examination. In this regard, the present proof-of-concept aligns with the broader move toward multimodal dermatologic diagnostics that combine minimally invasive sampling, structured imaging, and quantitative biomarker analysis [9,14–17].

5. Conclusions

The data support image-guided microbiopsy as the molecular component of a multimodal diagnostic workflow for skin ageing. Representative photography demonstrates a small visible footprint after sampling, skin-surface roughness imaging separates younger and older cohorts, and targeted qPCR identifies candidate biomarkers and multigene classifiers with encouraging accuracy. Together, these elements support further development of minimally invasive, imaging-linked molecular diagnostics in dermatology [1–5,7–17].

These results justify presenting the study to Diagnostics as a clinically oriented proof-of-concept manuscript, provided that the final submission confirms the exact analytical methods, ethics language, author information, and the identity of the fourth marker in the exploratory four-gene model.

 doi:10.20944/preprints202604.2019.v1

Institutional Review Board Statement: Approved by the University Human Research Ethics Committee (Approval No. 200017).

Informed Consent Statement: Informed consent was obtained from all subjects involved in the study.

Conflicts of Interest: TP owns shares of the Trajan Scientific and Medical which makes microbiopsies.

Acknowledgments: No acknowledgement.

References

1. Lin LL; Prow TW; Raphael AP; et al. Microbiopsy engineered for minimally invasive and suture-free sub-millimetre skin sampling. F1000Research 2013, 2, 120. doi:10.12688/f1000research.2-120.v1.
2. Lei BUW; Yamada M; Hoang VLT; et al. Absorbent microbiopsy sampling and RNA extraction for minimally invasive, simultaneous blood and skin analysis. Journal of Visualized Experiments 2020, (160), e61115. doi:10.3791/61115.
3. Jain M; Autuori I; Everett N; et al. Minimally invasive microbiopsy for genetic profiling of melanocytic lesions: a case series. Journal of the American Academy of Dermatology 2022, 86(6), 1338-1341. doi:10.1016/j.jaad.2021.05.018.
4. Churiso G; van Henten S; Cnops L; et al. Minimally invasive microbiopsies as an improved sampling method for the diagnosis of cutaneous leishmaniasis. Open Forum Infectious Diseases 2022, 9(6), ofac086. doi:10.1093/ofid/ofac086.
5. Wong QYA; Chew FT. Defining skin aging and its risk factors: a systematic review and meta-analysis. Scientific Reports 2021, 11, 22075. doi:10.1038/s41598-021-01573-z.
6. Glass D; Viñuela A; Davies MN; et al. Gene expression changes with age in skin, adipose tissue, blood and brain. Genome Biology 2013, 14, R75. doi:10.1186/gb-2013-14-7-r75.
7. Battistutta D; Pandeya N; Strutton GM; Fourtanier A; Tison S; Green AC. Skin surface topography grading is a valid measure of skin photoaging. Photodermatology, Photoimmunology & Photomedicine 2006, 22(1), 39-45. doi:10.1111/j.1600-0781.2006.00194.x.
8. Lagarde JM; Rouvrais C; Black D. Relation between skin micro-topography, roughness, and skin age. Skin Research and Technology 2015, 21(1), 69-76. doi:10.1111/srt.12160.
9. Sgouros D; Kouris A; Chrissopoulos A; et al. Dermoscopic assessment of xerosis severity, pigmentation pattern and vascular morphology in subjects with physiological aging and photoaging. Skin Research and Technology 2020, 26(1), 85-90. doi:10.1111/srt.12780.
10. Quan T. Molecular insights of human skin epidermal and dermal aging. Journal of Dermatological Science 2023, 112(2), 48-53. doi:10.1016/j.jdermsci.2023.08.006.
11. Jin S; Li K; Zong X; Eun S; Morimoto N; Guo S. Hallmarks of skin aging: update. Aging and Disease 2023, 14(6), 2167-2176. doi:10.14336/AD.2023.0321.
12. Raphael AP; Au V; Liew HM; et al. Clinical translation of scarless 0.33-mm core microbiopsy for molecular evaluation of human skin. Journal of the American Academy of Dermatology 2021, 84(1), 244-246. doi:10.1016/j.jaad.2020.06.1033.
13. Lee HJ; Kim M; Park J; et al. Microneedles: a novel clinical technology for evaluating skin characteristics. Skin Research and Technology 2024, 30(3), e13639. doi:10.1111/srt.13639.
14. Ruini C; Hartmann D; Schuh S; et al. Noninvasive multimodal imaging and its role in diagnosing skin lesions in dermatology: a systematic review and meta-analysis. JMIR Dermatology 2024, 7, e59666. doi:10.2196/59666.
15. Bossuyt PM; Reitsma JB; Bruns DE; et al. STARD 2015: an updated list of essential items for reporting diagnostic accuracy studies. Clinical Chemistry 2015, 61(12), 1446-1452. doi:10.1373/clinchem.2015.246280.
16. Cohen JF; Korevaar DA; Altman DG; et al. STARD 2015 guidelines for reporting diagnostic accuracy studies: explanation and elaboration. BMJ Open 2016, 6(11), e012799. doi:10.1136/bmjopen-2016-012799.
17. Bhat YJ; Islam MSU; Errichetti E. Ultraviolet-induced fluorescence dermoscopy, a novel diagnostic technique in dermatological practice: a systematic review. Indian Dermatology Online Journal 2025, 16(1), 25-39. doi:10.4103/idoj.idoj_299_24.

 doi:10.20944/preprints202604.2019.v1

18. Zou Z; Long X; Zhao Q; et al. A single-cell transcriptomic atlas of human skin aging. Developmental Cell 2021, 56(3), 383-397.e8. doi:10.1016/j.devcel.2020.11.002.
19. Lee JY; You J; Kim JY; et al. Novel gene expression profile of women with intrinsic skin youthfulness by whole transcriptome sequencing. International Journal of Molecular Sciences 2016, 17(10), 1587. doi:10.3390/ijms17101587.
20. Wyles SP; Allison DB; Ganier C; et al. SenSkin: a human skin-specific cellular senescence gene set. GeroScience 2025, 47, 1-18. doi:10.1007/s11357-025-01568-y.